

# Light-Activated Agonist-Potentiator of GABA<sub>A</sub> Receptors for Reversible Neuroinhibition in Wildtype Mice

Galyna Maleeva,<sup>+</sup> Alba Nin-Hill,<sup>+</sup> Ulrike Wirth, Karin Rustler, Matteo Ranucci, Ekin Opar, Carme Rovira, Piotr Bregestovski, Hanns Ulrich Zeilhofer, Burkhard König, Mercedes Alfonso-Prieto,<sup>\*</sup> and Pau Gorostiza<sup>\*</sup>



Cite This: *J. Am. Chem. Soc.* 2024, 146, 28822–28831



Read Online

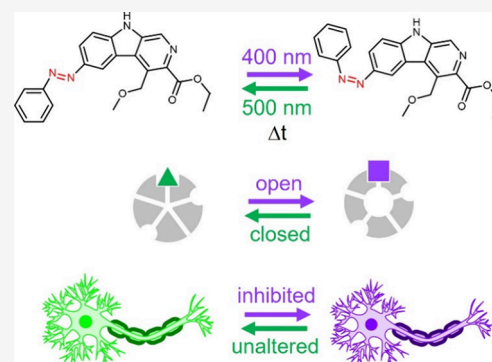
ACCESS |

Metrics & More

Article Recommendations

Supporting Information

**ABSTRACT:** Gamma aminobutyric acid type A receptors (GABA<sub>A</sub>Rs) play a key role in the mammalian central nervous system (CNS) as drivers of neuroinhibitory circuits, which are commonly targeted for therapeutic purposes with potentiator drugs. However, due to their widespread expression and strong inhibitory action, systemic pharmaceutical potentiation of GABA<sub>A</sub>Rs inevitably causes adverse effects regardless of the drug selectivity. Therefore, therapeutic guidelines must often limit or exclude clinically available GABA<sub>A</sub>R potentiators, despite their high efficacy, good biodistribution, and favorable molecular properties. One solution to this problem is to use drugs with light-dependent activity (photopharmacology) in combination with on-demand, localized illumination. However, a suitable light-activated potentiator of GABA<sub>A</sub>Rs has been elusive so far for use in wildtype mammals. We have met this need by developing azocarnil, a diffusible GABAergic agonist-potentiator based on the anxiolytic drug abecarnil that is inactive in the dark and activated by visible violet light. Azocarnil can be rapidly deactivated with green light and by thermal relaxation in the dark. We demonstrate that it selectively inhibits neuronal currents in hippocampal neurons *in vitro* and in the dorsal horns of the spinal cord of mice, decreasing the mechanical sensitivity as a function of illumination without displaying systemic adverse effects. Azocarnil expands the *in vivo* photopharmacological toolkit with a novel chemical scaffold and achieves a milestone toward future phototherapeutic applications to safely treat muscle spasms, pain, anxiety, sleep disorders, and epilepsy.



## INTRODUCTION

Gamma aminobutyric acid type A receptors (GABA<sub>A</sub>Rs) are the main inhibitory synaptic receptors in the mammalian central nervous system (CNS) and are important targets in pharmaceutical research.<sup>1</sup> They form heteropentameric transmembrane assemblies with a central chloride-ion-permeable pore that opens upon GABA binding, hyperpolarizing the cell membrane and inhibiting neuronal activity (Figure 1A). GABA<sub>A</sub>R agonists and potentiators (positive allosteric modulators, PAM) like barbiturates and especially benzodiazepines (Figure 1B), are widely used to treat muscle spasms, alcohol withdrawal, insomnia, anxiety, delirium, and seizures, as well as to induce sedation and anesthesia.<sup>2</sup> Propofol is a GABA<sub>A</sub>R PAM exclusively used for general anesthesia and binds to a different receptor site than benzodiazepines. GABA<sub>A</sub>R antagonists like bicuculline and gabazine are useful as research tools to functionally dissect neuronal GABA<sub>A</sub>R current components and behavioral phenotypes, but their stimulant and convulsant effects *in vivo* offer limited clinical applications, like treating benzodiazepine withdrawal syndrome and overdose.<sup>3</sup>

Neurons expressing GABA<sub>A</sub>Rs in the dorsal horns of the spinal cord are key elements in regulation of sensory

information and pain sensation. The complex local inhibitory circuitry in the dorsal horns is also known as the “gate” of peripheral sensory information.<sup>4</sup> Hence, downregulation of inhibitory transmission in this spinal cord region leads to the development of chronic pain.<sup>5</sup>

For these reasons, GABA<sub>A</sub>Rs in the spinal cord and other CNS regions have a privileged position as drivers of neuroinhibitory circuits that can be targeted for therapeutic purposes with potentiator drugs. However, due to their widespread expression and strong inhibitory action, systemic and indiscriminate potentiation of GABA<sub>A</sub>Rs with drugs gives rise to adverse effects regardless of the drug selectivity for these receptors. Therefore, despite the efficacy of clinically available GABA<sub>A</sub>R potentiators like phenobarbital and clonazepam, they are not recommended in modern therapeutic guidelines to treat neuropathic pain and to restore inhibitory drive in the

Received: June 23, 2024

Revised: September 24, 2024

Accepted: September 25, 2024

Published: October 9, 2024



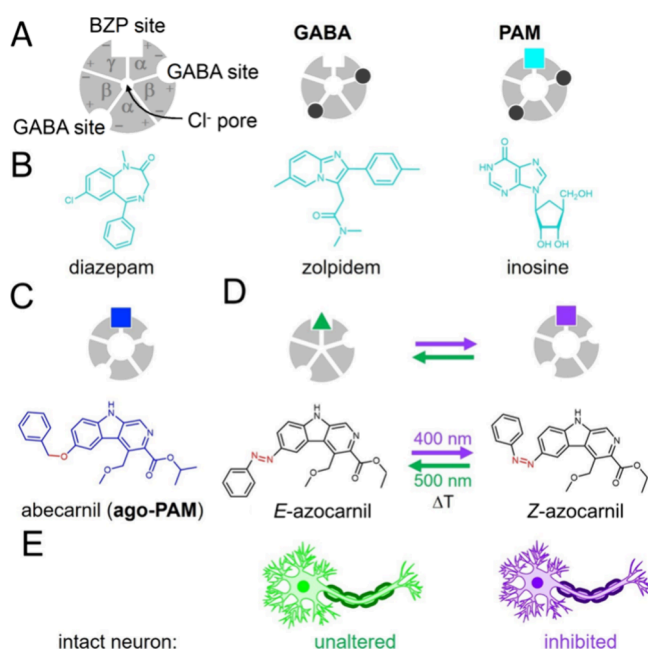


**Figure 1.** Design of a neuroinhibitory photoswitchable drug azocarnil. (A) Diagram of the GABA<sub>A</sub>R, as seen from the extracellular side, showing the subunit ( $\alpha$ ,  $\beta$ , and  $\gamma$ ) arrangement and the principal (+) and complementary (-) subunit interfaces, as well as the central Cl<sup>-</sup> ion pore, the orthosteric GABA ligand sites, and the primary allosteric ligand site of benzodiazepines (BZPs) and  $\beta$ -carbolines. Other allosteric potentiator sites (propofol, barbiturate, ethanol) are not shown for simplicity. Binding of the endogenous orthosteric ligand GABA (black dots) opens the Cl<sup>-</sup> permeable pore, thus hyperpolarizing (i.e., inhibiting the activity of) the neuron. Potentiators or positive allosteric modulators (PAMs, cyan square) enlarge Cl<sup>-</sup> currents, thus enhancing the inhibitory effect of GABA binding. (B) Examples of PAMs binding at the canonical high-affinity benzodiazepine binding site: diazepam, zolpidem,<sup>30</sup> and the endogenous GABA<sub>A</sub>R allosteric ligand inosine.<sup>31,32</sup> (C) A special class of PAMs (termed ago-PAMs, blue square) can open the ion channel in the absence of GABA, like abecarnil<sup>25,33</sup> below. (D) Design of a photoswitchable potentiator based on the structure of abecarnil by replacing the ether bond by an aza bond (azolog) and the isopropyl ester group by an ethyl ester group for synthetic accessibility reasons. Azobenzene photoisomerization between the *E* and *Z* configurations (represented as a green triangle and a violet square, respectively) is intended to change the agonist-potentiator activity and control GABA<sub>A</sub>R channel opening with light.  $\Delta T$  indicates the thermal relaxation from *Z* to *E* in the dark. (E) The activity of intact neurons can be modulated with light by means of their endogenous GABA<sub>A</sub>Rs and azocarnil applied in the medium. Neuronal activity should not be altered in the dark or under green light, corresponding to safe conditions regardless of the presence of the drug (e.g., systemically). Neuroinhibition should be elicited on demand and in localized regions using violet illumination.

spinal cord because they lead to intolerable systemic neuroinhibition in supraspinal CNS centers.<sup>6,7</sup>

One possibility to avoid undesired GABA<sub>A</sub>R potentiation at the systemic level while locally keeping it at the intended neuronal circuits (e.g., at the spinal cord for neuropathic pain) is to use drugs with light-dependent activity (photopharmacology) in combination with localized illumination. Drugs modified with chemical groups that change their configuration under different wavelengths of light have been shown to control protein activity, cell and tissue function,<sup>8</sup> and animal behavior.<sup>9</sup> These groups are dubbed photoswitches. One of

them is azobenzene, which reversibly photoisomerizes between *E* and *Z* configurations of its N=N double bond and changes its length and dipole moment.<sup>10</sup> These photoswitchable groups can be coupled by design to bioactive molecules with suitable pharmacological properties like agonism, antagonism, and modulation, thus producing powerful molecular tools to investigate physiological processes and to develop new therapeutic modalities.<sup>11</sup> A successful photopharmacological design strategy involves the direct replacement of biaryl amides or biaryl ethers by azobenzene (azobenzene analogs or “azologs”<sup>12,13</sup>) in a drug of interest, which endows the parent compound with photocontrolled activity while largely retaining all other valuable molecular properties.<sup>14</sup>

The ideal GABA<sub>A</sub>R photoswitchable drug profile for therapeutic purposes is the following: (1) It should have agonist-potentiator activity to provide robust neuroinhibition regardless of the presence of endogenous GABA, which may be reduced in certain conditions. (2) It should target the benzodiazepine site to avoid the anesthetic effects and the lack of analgesic action associated with the propofol site. (3) It should remain inactive in the dark to eliminate adverse effects at unintended locations in case that they are exposed to the drug (e.g., by systemic administration or diffusion from the local administration site). (4) It should be activated under illumination, preferably by visible light to avoid the cellular toxicity of UV light (<380 nm). (5) It should be a freely diffusible and drug-like small molecule to facilitate administration, biodistribution, and drug development.

Although considerable efforts have been invested to develop GABA<sub>A</sub>R photopharmacology (recently reviewed by Kramer and Rajappa<sup>15</sup>), the quest remains for a GABAergic photoswitchable agonist-potentiator that is inactive in the dark and demonstrates therapeutic effects in wildtype mammals under illumination. The only GABAergic compounds tested in mice so far are photoswitchable antagonists that must be covalently tethered to cysteine residues introduced in a GABA<sub>A</sub>R subunit by site-directed mutagenesis (optogenetic pharmacology).<sup>16,17</sup> Thus, they require using knock-in mice, which is advantageous for fundamental studies of inhibitory neurotransmission but not useful to develop therapeutic applications in wildtype animals, including humans. The tethered approach has also been applied to propofol agonists *in vitro*, including both dark-inactive<sup>18</sup> and dark-active<sup>19</sup> tethering sites. Besides, all freely diffusible GABA<sub>A</sub>R photoswitches that have been reported are dark-active (either targeting the channel pore,<sup>20</sup> the GABA site,<sup>21</sup> or the propofol site<sup>22</sup>) except for fulgazepam, a benzodiazepine modified with a fulgimide photoswitch that is dark-inactive and acts as a GABA<sub>A</sub>R potentiator under UV (365 nm) light.<sup>23</sup> Azopropofol displays anesthetic activity in tadpoles that is reduced under 360 nm light,<sup>22</sup> and fulgazepam allows photocontrolling zebrafish locomotion,<sup>23</sup> however, none of these ligands has been tested in rodents.

Thus, there is an unmet need for dark-inactive photoswitchable agonist potentiators of GABA<sub>A</sub>Rs to produce neuroinhibition with light in mammals. To achieve the photopharmacological profile outlined above, we focused on diffusible ligands targeting the benzodiazepine site, like fulgazepam,<sup>23</sup> but having a nonbenzodiazepine scaffold. We searched among  $\beta$ -carbolines,<sup>24</sup> which bind to the same site and produce similar pharmacological effects as benzodiazepines, and selected abecarnil<sup>25</sup> due to its drug-likeness and azologization potential (Figure 1C). Abecarnil acts as a partial agonist and PAM of GABA<sub>A</sub>Rs with high binding affinity.<sup>26</sup> It

shows anxiolytic and anticonvulsant effects, but in contrast to benzodiazepines, it exerts weak or no sedative and ataxic actions.<sup>27–29</sup>

We designed an azobenzene analogue of abecarnil (termed azocarnil) by replacing the ether bond by an azo group (Figure 1C). In the absence of the receptor-bound atomic structure of abecarnil, we used molecular docking calculations to test whether such modification is compatible with receptor binding and whether there are differences in binding between the *Z* and *E* isomers. Our computational results suggested that *Z*-azocarnil, but not *E*, can bind in the benzodiazepine site similar to abecarnil and diazepam. Such a prediction is confirmed by our experimental observation that azocarnil potentiates GABAergic currents in hippocampal neurons under 400 nm illumination (*Z* configuration). Upon intrathecal injection in wildtype mice, azocarnil decreases the withdrawal responses to cutaneous mechanical stimulation as a function of spinal cord illumination and does not display systemic adverse effects. Thus, photoswitchable analogs of abecarnil significantly expand the GABA<sub>A</sub>R photopharmacological toolkit based on a novel chemical scaffold and achieve photoactivated neuroinhibition without adverse effects in mammals, a milestone toward future therapeutic applications to safely treat muscle spasms, pain, anxiety and sleep disorders, and epilepsy.

## RESULTS

**Molecular Design of a Photoactivated Agonist-Potentiator of GABA<sub>A</sub>Rs.** We started by asking whether azocarnil retains the binding properties of abecarnil and whether the properties can be controlled by *Z–E* photoisomerization. Since the GABA<sub>A</sub>R structure bound to abecarnil is not available, we looked for other compounds that bind to the same receptor site and whose structure in complex with GABA<sub>A</sub>R has been determined experimentally, with the aim of using molecular docking calculations to compare them. We first validated our docking protocol by redocking methyl 6,7-dimethoxy-4-ethyl- $\beta$ -carboline-3-carboxylate (DMCM, a negative allosteric modulator of the same  $\beta$ -carboline family as abecarnil, Figure 2A) and diazepam (another potentiator binding to the same site but from the benzodiazepine family, Figure 2B) in their respective cryo-electron microscopy structures in complex with the human GABA<sub>A</sub>R  $\alpha_1\beta_2\gamma_2$  subtype (PDB codes 8DD3<sup>34</sup> and 6X3X,<sup>35</sup> respectively). The representative docking poses obtained are almost identical with the experimentally determined binding poses for both ligands (Figure S6), confirming the reliability of the docking protocol used.

We then computed the binding mode of the parent compound abecarnil (potentiator), focusing on the benzodiazepine binding site between the principal (+) side of the  $\alpha_1$  subunit and the complementary (–) side of the  $\gamma_2$  subunit, as this is the known primary, high-affinity site for both  $\beta$ -carbolines and benzodiazepines in GABA<sub>A</sub>Rs.<sup>24,26</sup> Most of the experimentally observed interactions for diazepam and DMCM are retained for abecarnil (Table S1). We also observe that the phenyl pendant ring of abecarnil is placed in the same region as the phenyl pendant ring of diazepam and the phenyl ring of DMCM. This region contains most of the residues for which mutagenesis data is available, demonstrating their importance for  $\beta$ -carboline and benzodiazepine binding.<sup>34,36–40</sup>

To evaluate the feasibility that azocarnil maintains the same binding mode as the parent compound abecarnil in the benzodiazepine site, we then performed molecular docking

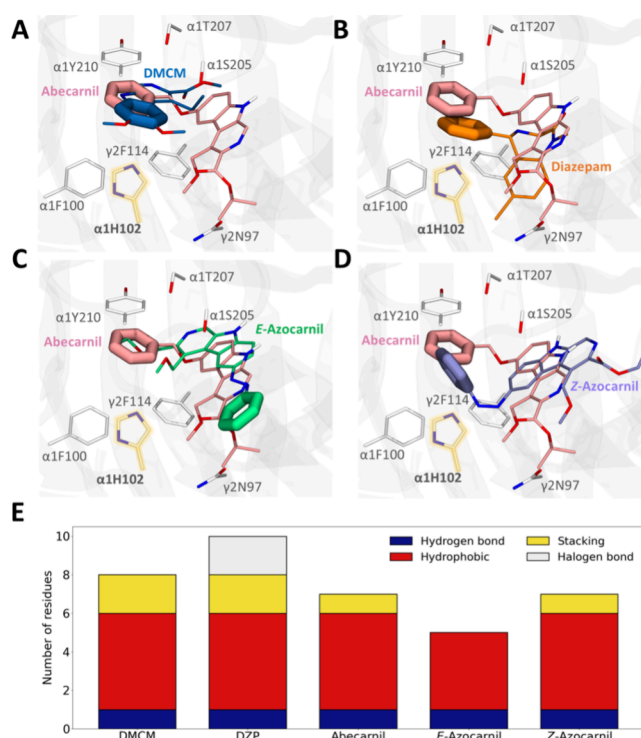


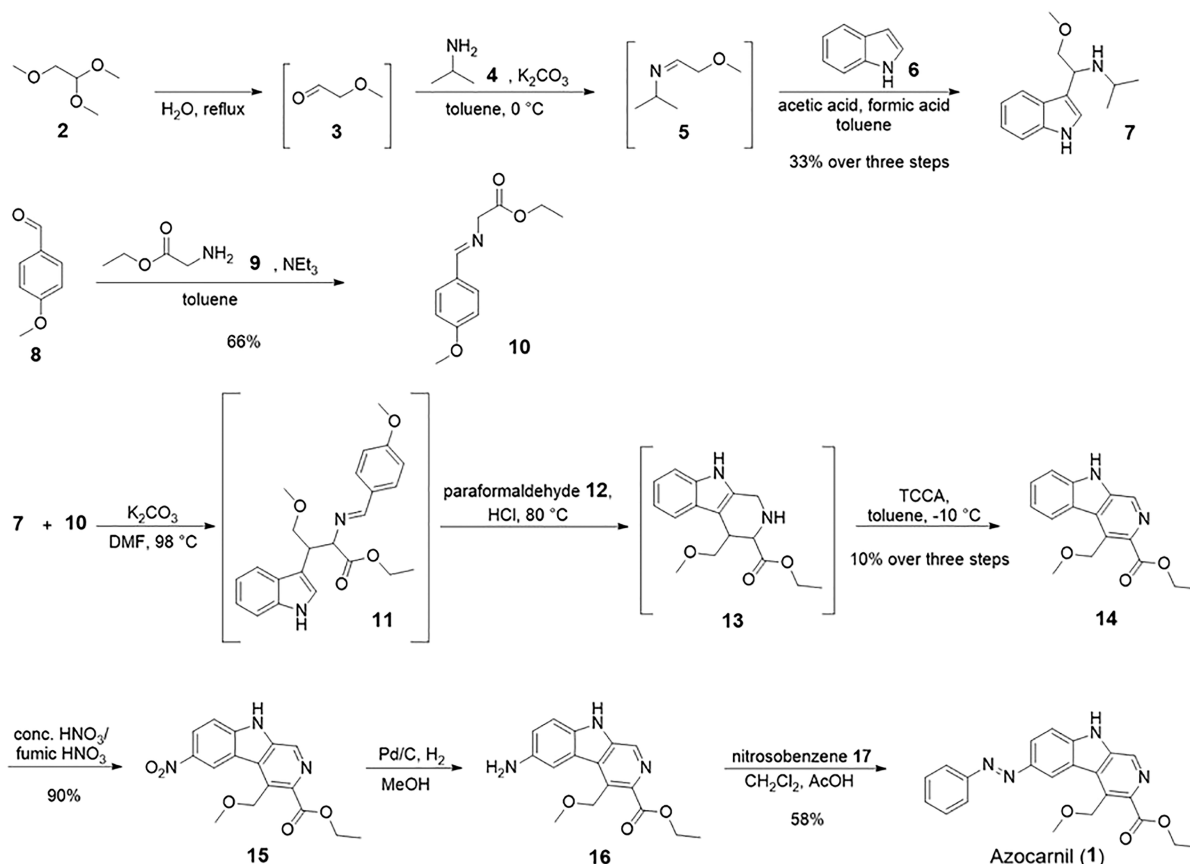
**Figure 2.** Molecular docking calculations of abecarnil and *E*- and *Z*-azocarnil in the benzodiazepine binding site of the GABA<sub>A</sub> receptor. Comparison of the representative docking pose of the most populated cluster between abecarnil (pink) and (A) DMCM (blue, experimental structure with PDB code 8DD3), (B) diazepam (orange, experimental structure with PDB code 6X3X), (C) *E*-azocarnil (green), and (D) *Z*-azocarnil (violet). Only the GABA<sub>A</sub>R residues (white sticks) for which mutagenesis data is available are shown.<sup>34,36–40,42</sup> The  $\alpha_1$  His102 residue (Table S1 and Figures S3–S5), which is essential for  $\beta$ -carboline activity, is highlighted in yellow.<sup>37</sup> The phenyl rings of the compounds are shown as thicker lines to emphasize their positions in the benzodiazepine site. (E) Number of GABA<sub>A</sub>R residues for which mutagenesis data are available that are in contact with the compounds, quantifying separately hydrogen bond (dark blue), hydrophobic (red), stacking (yellow), and halogen bond (gray) interactions.

calculations of both *E* and *Z* isomers, as previously done for other photoswitchable ligands targeting GABA<sub>A</sub>Rs.<sup>41</sup> The orientation of the docked *E*-azocarnil does not resemble abecarnil, diazepam, or DMCM, as it is turned around 180° (Figure 2C). Moreover, the *E* form is missing a key interaction with the  $\alpha_1$  His102 residue (Table S1 and Figure S4B), which is essential for  $\beta$ -carboline activity according to mutagenesis data.<sup>37</sup> In contrast, the preferred binding pose of docked *Z*-azocarnil resembles that of docked abecarnil (Figure 2D), as well as that of diazepam and DMCM. The azobenzene moiety of *Z*-azocarnil is superimposed with the pendant phenyl ring of the diazepam molecule, thus conserving the strong stabilization by the surrounding aromatic residues<sup>35</sup> (Figures 2E and S4A). Altogether, the binding modes predicted by docking in the benzodiazepine binding site suggest that *Z*-azocarnil could act as a potentiator. To test this prediction experimentally, we proceeded with the synthesis of azocarnil and the characterization of its photopharmacological properties.

**Synthesis of Azocarnil.** To design a photoswitchable analogue of abecarnil (Figure 1C), the ether bond between the carboline scaffold and the pendant phenyl ring was replaced by an azo group, and the isopropyl ester group had to be



Scheme 1. Synthetic Route toward Azocarnil (1)



substituted by an ethyl ester group for synthetic accessibility reasons. The synthetic approach (Scheme 1) to the resulting compound (azocarnil, **1**) started from 1,1,2-trimethoxyethane (**2**) which was hydrolyzed to afford methoxyacetaldehyde (**3**) which was, due to its thermal instability and volatility, directly used in the reaction with isopropylamine (**4**) to form **5**. Intermediate **5** was, without further purification, reacted with indole (**6**) to give compound **7**. In a reaction executed in parallel, the reaction of 4-methoxybenzaldehyde (**8**) and glycine ethyl ester (**9**) gave imine **10**. The three-step synthesis toward  $\beta$ -carboline **14** starting from **7** and **10**, including the cyclization with paraformaldehyde (**12**) in a Pictet-Spengler reaction and oxidation with trichloroisocyanuric acid (TCCA) to obtain the fully aromatic scaffold, was done in one pot without isolation of the intermediates **11** and **13**. The next step involved the nitration of **14** with a mixture of concentrated and fuming nitric acid to get nitro compound **15**. Subsequent reduction of the nitro group led to amine **16**. The photochromic moiety of **1** was introduced in the last step by performing a Mills reaction using nitrosobenzene (**17**) and the amine **16** in acetic acid.

**Photochemical Properties of Azocarnil.** The photochemical properties of azocarnil were characterized by using absorption spectroscopy in DMSO and aqueous buffer. It can be toggled reversibly between its *Z*- and *E*-isomer using LEDs emitting 400 nm violet light and 505 nm green light, respectively (Figure S8A). The *E*-isomer absorption plot is colored green and shows the typical azobenzene absorption maximum at 360 nm. Upon switching under 400 nm light during 1 min, a new maximum at 450 nm appears

corresponding to the *Z*-isomer (violet in Figure S8A). Azocarnil displays a high fatigue resistance in DMSO and water (Figure 3B). The thermal relaxation half-life in DMSO is 10.4 h (lifetime 15 h, rate  $0.07 \text{ h}^{-1}$ ), which allows for investigating the photostationary states (PSS) by HPLC (Figure S8C). It exhibits a PSS of 87% *Z* for the *E*- to *Z*-isomerization after 400 nm light and 25% *Z* for the *Z*- to *E*-isomerization after 505 nm light. The thermal relaxation half-life of azocarnil in aqueous buffer is 1.5 min (lifetime 2.1 min, rate  $0.47 \text{ min}^{-1}$ , Figure S8C). Hence, the PSS could not be determined by HPLC or NMR. In the next sections, *Z*-azocarnil refers to the maximum *Z* isomer fraction at the PSS under 400 nm illumination, and *E*-azocarnil refers to the maximum *E* isomer fraction at the PSS under 505 nm illumination. After thermal relaxation in the dark, azocarnil solutions are 100% *E*.

**Azocarnil is a Light-Activated GABAergic Agonist-Potentiator *in Vitro*.** We next evaluated the photopharmacological properties of the compound *in vitro* using whole cell patch clamp electrophysiology in hippocampal neurons under different illumination conditions. We chose primary neurons because they express a representative diversity of physiological GABA<sub>A</sub>R subunits and heteropentameric subtypes, in contrast to overexpressed receptors in cell lines or oocytes, which provide specific receptor responses but involve longer screening processes and can lead to nonphysiologically relevant results.<sup>43,44</sup> Thus, we tested the effect of *E*- and *Z*-azocarnil on endogenous GABA<sub>A</sub>Rs in cultured neurons by measuring whole-cell macroscopic currents and transient miniature inhibitory postsynaptic currents (mIPSCs). When voltage

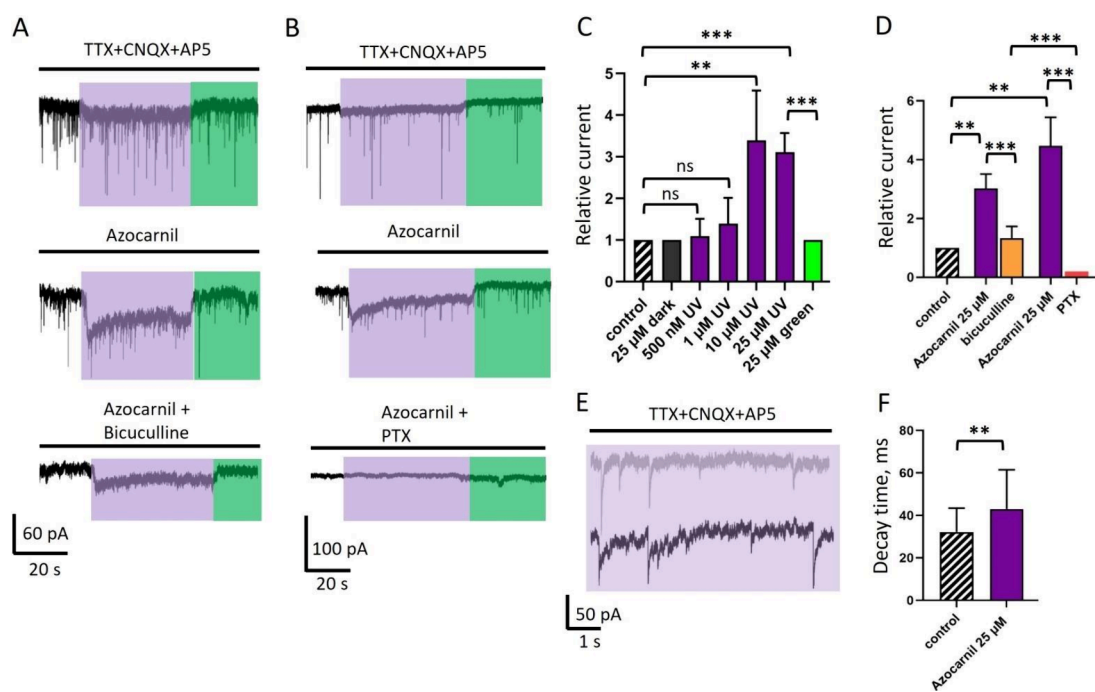


**Figure 3.** Effect of azocarnil on endogenous GABAergic currents in cultured primary hippocampal neurons. (A) Voltage-clamp recordings of GABAergic currents (represented in pA units, see scale bar at the bottom of the panel) in control conditions (TTX 1  $\mu$ M to block voltage-dependent sodium channels, CNQX 10  $\mu$ M, and AP5 40  $\mu$ M to block glutamatergic currents), after application of azocarnil (10  $\mu$ M), and after addition of bicuculline (25  $\mu$ M, competitive antagonist of the GABA site in GABA<sub>A</sub>Rs). Illumination with 400 and 500 nm light is depicted by violet and green boxes, respectively.  $V_{\text{hold}} = -70$  mV. (B) GABAergic currents in the control, after addition of azocarnil (25  $\mu$ M) and after addition of the GABA<sub>A</sub>R pore blocker picrotoxin (PTX, 100  $\mu$ M). (C) Cumulative graph demonstrating the relative mean amplitude of macroscopic GABAergic currents recorded during simultaneous application of different concentrations of azocarnil and 400 nm illumination. Here and elsewhere the values represent mean  $\pm$  SD. Comparison was done using a paired  $t$  test,  $n = 5-7$  cells for each concentration; ns, not significant; \*\*,  $P < 0.01$ ; \*\*\*,  $P < 0.001$ . (D) Cumulative graph showing the mean amplitude of macroscopic GABAergic currents in two different sets of experiments: when current induced by application of azocarnil (25  $\mu$ M) and 400 nm light was inhibited by bicuculline (25  $\mu$ M; orange column) and by PTX (100  $\mu$ M; red column). (E) Azocarnil (25  $\mu$ M) under 400 nm light increases the decay time of the mIPSCs. Recording of mIPSCs at 400 nm illumination in control conditions (gray trace) and mIPSCs at 400 nm illumination combined with the application of azocarnil (25  $\mu$ M, black trace). (F) Cumulative graph demonstrating the effect of azocarnil (25  $\mu$ M) combined with 400 nm light on the decay time (ms) of mIPSCs in cultured hippocampal neurons. Comparison was done using an unpaired  $t$  test,  $n = 78$  events from 4 independent experiments; \*\*,  $P < 0.001$ . TTX: tetrodotoxin (voltage-gated sodium channel blocker). CNQX: 6-cyano-7-nitroquinoxaline-2,3-dione (AMPA receptor antagonist). AP5: (2R)-amino-5-phosphonovaleric acid (NMDA receptor antagonist).

clamped neurons are illuminated at 400 nm in the absence of the compound (control conditions), a small but noticeable deflection of the baseline is observed (Figure 3A,B, upper panels). To take into account this baseline photocurrent in the quantifications for every cell, we recorded it under 400 and 500 nm before the application of azocarnil, and all currents measured at the peak of the response were normalized to this baseline.

Upon perfusion of 500 nM to 25  $\mu$ M azocarnil in the absence of illumination, the current did not change significantly. When cells were illuminated with 400 nm light during azocarnil perfusion, the magnitude of the photocurrent exceeded the baseline photocurrent. At 500 nM to 1  $\mu$ M azocarnil, the relative amplitude of GABAergic currents under 400 nm light increased nonsignificantly by a factor of  $1.1 \pm 0.4$  ( $n = 7$  cells) and  $1.4 \pm 0.6$  ( $n = 6$  cells), respectively (paired  $t$  test). When azocarnil concentration was raised to 10  $\mu$ M and 25  $\mu$ M, the macroscopic GABAergic currents increased significantly by a factor of  $3.4 \pm 1.2$  ( $n = 7$  cells,  $P < 0.01$ , 10  $\mu$ M) and  $3.1 \pm 0.5$  from control ( $n = 5$  cells,  $P < 0.001$ , 25  $\mu$ M) as shown in Figure 3A,C. Upon application of the vehicle (DMSO 0.5%) and 400 nm illumination, macroscopic currents were of the same amplitude as baseline photocurrents, and the

kinetics of synaptic GABAergic currents was not altered (Figure S11D), confirming the specificity of the azocarnil effect.

To confirm that the recorded currents have GABAergic origin, after every experiment, we applied bicuculline, a GABA<sub>A</sub>R inhibitor antagonizing the GABA site (Figure 3A,D). The application of bicuculline completely suppressed GABAergic mIPSCs and partially but significantly inhibited the macroscopic photocurrents to a factor of  $1.3 \pm 0.4$  from the control ( $n = 4$ ; Figure 3A,D). Note that, in contrast to the photocurrent baseline in the absence of azocarnil, the characteristic time course of the GABAergic macroscopic photocurrent with a desensitizing component is retained in the presence of azocarnil and bicuculline (Figure 3A). In a separate set of experiments after recording GABAergic currents, we applied the GABA<sub>A</sub>R pore blocker picrotoxin (PTX, 100  $\mu$ M) and observed a complete suppression of both the mIPSCs and the macroscopic GABAergic photocurrents induced by *Z* azocarnil (Figure 3B,D). The partial inhibition of photocurrents by bicuculline (which displaces GABA from its binding sites, thus suppressing any potentiator effects) reveals an agonist-like activity of azocarnil. In contrast, PTX abolishes both the agonist and potentiator effects of azocarnil, which

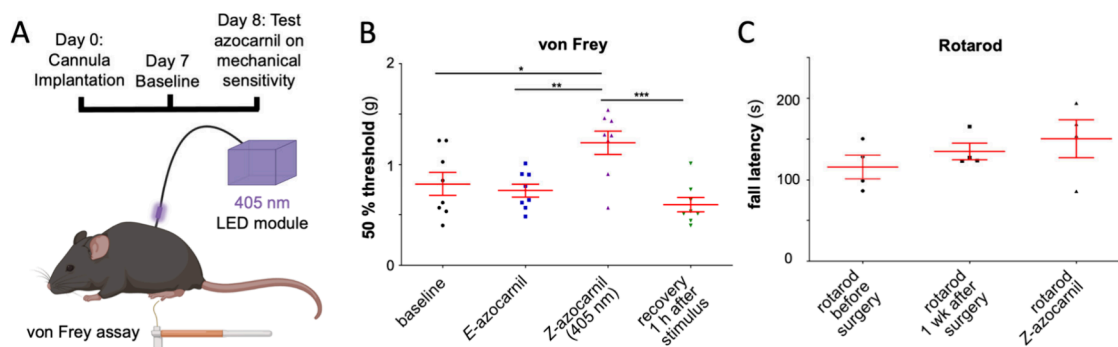


**Figure 4.** Azocarnil exerts photoactivated neuroinhibition in mice. (A) Experimental setup to measure changes in mechanical sensitivity using the von Frey filament test. Photoactivation of *E*-azocarnil was done with UV light of 405 nm (10–20  $\mu$ W) delivered by an optical fiber connected to the lumbar spine. (B) Withdrawal thresholds measured at baseline (7 days after cannula implantation, 20 min after intrathecal injection of azocarnil (300  $\mu$ M; 10  $\mu$ L), during violet illumination (405 nm; 10–20  $\mu$ W), and 1 h after violet light was turned off). (C) Motor coordination assessed in the rotarod test. Each data point represents one mouse. Red lines show mean and SEM \*,  $P < 0.05$ , \*\*  $P < 0.01$ , \*\*\*  $P < 0.001$ . One-way ANOVA followed by Bonferroni posthoc test. Figure 4A was created using the free version of BioRender (<https://www.biorender.com>).

corresponds to a pore blocker effect. Note that the different effects of 25  $\mu$ M azocarnil between the experiments to separately test bicuculline and PTX on the photoresponses (Figure 3D) are due to differences across individual neurons and neuronal cultures (we used 7 different animals and hippocampal dissections, which include heterogeneous neuronal populations and protein expression profiles like GABA<sub>A</sub>Rs).

We also studied the decay time of the mIPSCs under 400 nm illumination before and after azocarnil application and observed a statistically significant increase at 25  $\mu$ M, from  $32 \pm 11$  ms to  $43 \pm 19$  ms (Figure 3 EF;  $P < 0.01$ ,  $n = 78$  events from 4 independent experiments).

In addition, we investigated the effect of azocarnil on glutamatergic miniature excitatory postsynaptic currents (mEPSCs). Application of azocarnil in combination with 400 or 500 nm light did not induce changes in either the amplitude of the macroscopic current (Figure S11A) or the decay time of the mEPSCs (Figure S11B,C).

Together, electrophysiological and pharmacological experiments in hippocampal neurons demonstrate that azocarnil is inactive in the dark and that it acts as a micromolar agonist-potentiator of GABA<sub>A</sub>Rs under 400 nm light, producing macroscopic GABAergic currents and prolonging the decay kinetics of synaptic mIPSCs.

**Azocarnil Can Be Safely Injected and Photocontrols Mechanical Sensitivity *in Vivo*.** We next tested the effect of photoactivated azocarnil on spinal nociception *in vivo*. The spinal cord dorsal horn is the first site of synaptic processing in pain pathways. At this site, sensory information conveyed by peripheral nerve fibers is processed by a local network consisting of excitatory glutamatergic and inhibitory GABAergic (and glycinergic) neurons before it is relayed to higher central nervous system areas. The magnitude of aversive responses triggered by cutaneous mechanical stimulation strongly depends on the activity of inhibitory (GABAergic and glycinergic) interneurons of the spinal cord.<sup>45</sup>

The sensitivity of mice to mechanical stimulation of the plantar side of the left hind paw was assessed with von Frey filaments (for a schematic presentation of the experimental design, see Figure 4A). The first baseline measurement was taken 7 days after cannula implantation. On the following day, a second baseline was taken 20 min after *E*-azocarnil was injected intrathecally (i.e., into the cerebrospinal fluid). *E*-Azocarnil did not cause any significant change relative to the

baseline sensitivity (Figure 4B). Photoactivation of *E*-azocarnil was started immediately after, by delivering violet light (405 nm, 10–20  $\mu$ W) on the dorsal side of the lumbar spinal cord at levels L4/L5 through an optical fiber. At this stage, the von Frey filament test was performed during continuous light stimulation, showing a significant decrease in the mechanical sensitivity (Figure 4B). Illumination was then discontinued, and motor coordination was subsequently assessed. No change in the rotarod performance was observed (Figure 4C). The von Frey filament test was performed again 1 h after the illumination was stopped, showing a recovery to baseline mechanical sensitivity (Figure 4B).

Overall, azocarnil achieves a qualitative advancement in the photopharmacology of GABA<sub>A</sub>Rs due to its unique properties. Its agonist-potentiator activity provides robust neuroinhibition independently of GABA. Our molecular modeling results predict that azocarnil retains binding to the benzodiazepine site and that it establishes stronger receptor-drug interactions in the illuminated *Z* form than in the dark-relaxed *E* form. Accordingly, azocarnil has lower GABA<sub>A</sub>R activity in the dark, it is photoactivated by visible violet light *in vitro* and *in vivo*, and it does not produce systemic adverse effects when injected intrathecally in mice. Thus, azocarnil is a freely diffusible and drug-like small molecule photoswitch that is amenable to further development for therapeutic purposes in which on-demand and localized neuroinhibition is required.

We have demonstrated that under 400 nm illumination azocarnil induces macroscopic GABAergic current and prolongs the decay time of synaptic currents in cultured hippocampal neurons (Figure 3). These effects are specific to GABA<sub>A</sub>Rs and do not alter glutamatergic currents (Figure S11ABC). Visible light of 400 nm can alter retinal and cortical neurons,<sup>46</sup> but unlike UV light, it does not damage nucleic acids or produce reactive oxygen species.<sup>47</sup> Azocarnil is about 100-fold less potent than abecarnil,<sup>48</sup> as it is sometimes found in photopharmacology.<sup>23</sup> Considering the excellent performance of azocarnil *in vitro*, we tested it to control the transmission of sensory information in the spinal cord *in vivo*. We observed that 405 nm light delivered to the lumbar spine after intrathecal injection of azocarnil significantly decreases the hind paw sensitivity in the von Frey test without affecting motor coordination (Figure 4). Thus, it is a photoactivated potentiator of GABAergic neurotransmission



that efficiently controls mechanical sensitivity without adverse effects.

Compared to other reported diffusible photoswitches, azocarnil is less potent than the antagonist azogabazine but ten times more potent than other photoswitchable GABA<sub>A</sub>R potentiators like MPC088, AP-2, and fulgazepam.<sup>21–23</sup> In contrast to the propofol derivatives MPC088 and AP-2, it is inactive in the dark. Azocarnil is also more synthetically accessible than fulgazepam<sup>23</sup> and constitutes the first GABA<sub>A</sub>R photoswitch activated by visible light, allowing the use of compact 405 nm laser diodes.

Azocarnil does not induce anesthesia at the doses studied here (Figure 4C), in contrast to the action of propofol. This result agrees with the properties of benzodiazepine site ligands. However, the observed changes in the receptor decay kinetics (Figure 3D,E) diverge from the canonical benzodiazepine mechanism<sup>49</sup> and may involve secondary binding sites<sup>50,51</sup> that require further studies.

The photoactivation of azocarnil with visible light and its prominent effect on mechanical sensitivity make it eligible for selective, on-demand, and localized inhibition of pathologic pain signaling at the dorsal horn of the spinal cord. Peripheral neuropathic pain involves the release of inflammatory molecules that alter the activity of a wide variety of targets on dorsal root ganglion neurons, including voltage gated ion channels (Na<sub>v</sub>, K<sub>v</sub>, Ca<sub>v</sub>) and GABA<sub>A</sub>Rs, among others.<sup>52</sup> However, drugs targeting the latter are not used clinically to treat pain due to their systemic adverse effects. Several studies have been published to control pain *in vivo* with photopharmacology.<sup>53–58</sup> A photoswitchable adenosine receptor agonist decreases the inflammatory pain when injected locally in the affected paw. However, it is active in the dark and deactivated under illumination, which limits its usability.<sup>53</sup> Several photoswitchable modulators of metabotropic glutamate receptors can be used to treat inflammatory and neuropathic pain *in vivo*, but they require highly invasive injections in the brain and are also dark-active.<sup>54–57</sup> A photoswitchable carbamazepine (carbadiazocine) for neuropathic pain is also active in the dark.<sup>58</sup> None of them can take advantage of the GABAergic gate of sensory information in the dorsal horn like azocarnil, which is poised as a promising photopharmacological drug candidate against pathological pain.

For that purpose, the molecular properties of azocarnil that can be improved include the activation wavelength, which has a low penetration in tissue. Photoactivation with orange-red light would be convenient, and azobenzene substitutions to achieve it have been described;<sup>59</sup> however, they involve bulky substituents that may affect azocarnil potency, drug-likeness, and the prospects of oral bioavailability and CNS exposure derived from abecarnil. The lack of adverse systemic effects of azocarnil after intrathecal injection and localized illumination (Figure 4) prompts future pharmacokinetic studies by other routes of administration that give good tolerability and efficacy in humans with abecarnil.<sup>60,61</sup>

## CONCLUSIONS

To address the need for photoswitchable GABAergic drugs for therapies with high efficacy and without adverse effects, we developed azocarnil, a small molecule photoswitchable analogue of the drug abecarnil. This compound overcomes several limitations of previously reported photoswitchable GABAergic ligands. It is an agonist-potentiator of GABA<sub>A</sub>Rs that is inactive in the dark and can be activated with visible

light and with precise spatiotemporal selectivity, both in hippocampal neurons and in the dorsal horns of the spinal cord of mice. Azocarnil is the first diffusible GABAergic photoswitch that is demonstrated in wildtype mammals, achieving a prominent decrease in their sensitivity to touch without concomitant motor effects.

## ASSOCIATED CONTENT

### Data Availability Statement

The datasets generated and analyzed during the current study are available from the corresponding authors on reasonable request.

### Supporting Information

The Supporting Information is available free of charge at <https://pubs.acs.org/doi/10.1021/jacs.4c08446>.

Further details on the experimental and computational procedures used in this study, spanning molecular modeling, synthesis and analytical characterization of azocarnil, and electrophysiological characterization in neuronal cell cultures and mice experiments. Additional figures and tables supplementing the results presented in the main text, including validation of the docking protocol, photophysical and NMR characterization and electrophysiological control recordings (PDF)

## AUTHOR INFORMATION

### Corresponding Authors

**Mercedes Alfonso-Prieto** – Institute of Neuroscience and Medicine INM-9 Computational Biomedicine, Forschungszentrum Jülich GmbH, D-52428 Jülich, Germany; [orcid.org/0000-0003-4509-4517](https://orcid.org/0000-0003-4509-4517); Email: [m.alfonso-prieto@fz-juelich.de](mailto:m.alfonso-prieto@fz-juelich.de)

**Pau Gorostiza** – Catalan Institution for Research and Advanced Studies (ICREA), Barcelona 08010, Spain; Institute for Bioengineering of Catalonia (IBEC), The Barcelona Institute for Science and Technology, Barcelona 08028, Spain; Networking Biomedical Center in Bioengineering, Biomaterials, and Nanomedicine (CIBER-BBN), ISCIII, Barcelona 08028, Spain; [orcid.org/0000-0002-7268-5577](https://orcid.org/0000-0002-7268-5577); Email: [pau@icrea.cat](mailto:pau@icrea.cat)

### Authors

**Galyna Maleeva** – Institute for Bioengineering of Catalonia (IBEC), The Barcelona Institute for Science and Technology, Barcelona 08028, Spain; Networking Biomedical Center in Bioengineering, Biomaterials, and Nanomedicine (CIBER-BBN), ISCIII, Barcelona 08028, Spain

**Alba Nin-Hill** – Departament de Química Inorgànica i Orgànica (Secció de Química Orgànica) & Institut de Química Teòrica i Computacional (IQTUCB), Universitat de Barcelona, Barcelona 08020, Spain; Present Address: Toulouse Biotechnology Institute, TBI, Université de Toulouse, CNRS, INRAE, INSA, F-31077 Toulouse Cedex, France; [orcid.org/0000-0002-8670-9031](https://orcid.org/0000-0002-8670-9031)

**Ulrike Wirth** – Institute of Organic Chemistry, University of Regensburg, Regensburg 93053, Germany

**Karin Rustler** – Institute of Organic Chemistry, University of Regensburg, Regensburg 93053, Germany; Present Address: Iris Biotech GmbH, Marktredwitz, 95615 Germany

Matteo Ranucci – Institute of Pharmacology and Toxicology, University of Zurich, Zürich 8057, Switzerland

Ekin Opar – Institute for Bioengineering of Catalonia (IBEC), The Barcelona Institute for Science and Technology, Barcelona 08028, Spain; Networking Biomedical Center in Bioengineering, Biomaterials, and Nanomedicine (CIBER-BBN), ISCIII, Barcelona 08028, Spain; Doctorate program of the University of Barcelona, Barcelona 08020, Spain

Carme Rovira – Departament de Química Inorgànica i Orgànica (Secció de Química Orgànica) & Institut de Química Teòrica i Computacional (IQTCUB), Universitat de Barcelona, Barcelona 08020, Spain; Catalan Institution for Research and Advanced Studies (ICREA), Barcelona 08010, Spain; [orcid.org/0000-0003-1477-5010](https://orcid.org/0000-0003-1477-5010)

Piotr Bregestovski – Institut de Neurosciences des Systèmes, UMR INSERM 1106, Aix-Marseille Université, Marseille 13005, France; Present Address: Institute of Neuroscience, Kazan State Medical University, Kazan, 420012 Russia

Hanns Ulrich Zeilhofer – Institute of Pharmacology and Toxicology, University of Zurich, Zürich 8057, Switzerland; Institute of Pharmaceutical Sciences, Swiss Federal Institute of Technology (ETH) Zürich, Zürich 8093, Switzerland

Burkhard König – Institute of Organic Chemistry, University of Regensburg, Regensburg 93053, Germany; [orcid.org/0000-0002-6131-4850](https://orcid.org/0000-0002-6131-4850)

Complete contact information is available at:  
<https://pubs.acs.org/10.1021/jacs.4c08446>

#### Author Contributions

\*G.M. and A.N.-H. contributed equally.

#### Notes

The authors declare no competing financial interest.

#### ACKNOWLEDGMENTS

This research was funded by the EU Horizon 2020 Framework Programme for Research and Innovation, including the European Innovation Council Pathfinder (Phototheraport, 101130883), Human Brain Project (WaveScaleS, SGA3, 945539), ERA SynBio Grant MODULIGHTOR (PCIN-2015-163-C02-01), and Information and Communication Technologies (Deeper, ICT-36-2020-101016787). It was also supported by the Government of Catalonia (CERCA Programme; AGAUR 2021-SGR-01410 to P.G. and 2021-SGR-00680 to C.R.); by the Spanish Ministry of Science and Innovation (DEEP RED, grant PID2019-111493RB-I00; EPILLUM, grant AEI/10.13039/501100011033; Research Network in Biomedicine eBrains-Spain, RED2022-134823-E; and MICINN/AEI/FEDER, UE, PID2020-118893GB-I00, to C.R.); the Spanish Structures of Excellence María de Maeztu (CEX2021-001202-M, to C.R. and A.N.-H.); and in part by the DFG Research Unit FOR2518 “Functional Dynamics of Ion Channels and Transporters – DynIon” (project P6, AL 2511/1-2 to M.A.-P). G.M. was supported by a Ramón y Cajal Investigator grant (RYC2021-033056-I financed by MCIN/AEI/10.13039/501100011033 and by the European Union NextGeneration EU/PRTR). This study has also benefitted from the postdoctoral fellowship Margarita Salas (A.N.-H.) funded by the Spanish Ministry of Science, Innovation and Universities (MICIU). Part of the work presented here has been adapted from the PhD dissertation of U.W. (“Photochromic Molecules for Biological Applications”, University of Regensburg, Germany, 2024), under a CC BY 4.0 license.

Permission for all animal experiments was obtained from the Kanton of Zurich (license 097/2021). All animal experiments complied with the relevant ethical regulations.

#### ABBREVIATIONS

AcOH	acetic acid
AMPA receptor	$\alpha$ -amino-3-hydroxy-5-methyl-4-isoxazole-propionic acid receptor
AP5	(2R)-amino-5-phosphonovaleric acid
ATP	adenosine triphosphate
CNQX	6-cyano-7-nitroquinoxaline-2,3-dione
DIV	days in vitro
DMCM	methyl 6,7-dimethoxy-4-ethyl- $\beta$ -carboline-3-carboxylate
DMSO	dimethyl sulfoxide
EGTA	ethylene glycol-bis( $\beta$ -aminoethyl ether)- $N,N,N',N'$ -tetraacetic acid
GABA	$\gamma$ -aminobutyric acid
GTP	guanosine-5'-triphosphate
HPLC	high performance liquid chromatography
mEPSCs	miniature excitatory postsynaptic currents
mIPSCs	miniature inhibitory postsynaptic currents
ms	millisecond
NMDA receptor	$N$ -methyl-D-aspartate receptor
NMR	nuclear magnetic resonance
pA	picoampere
PAM	positive allosteric modulator
PDB	protein data bank
PE	petroleum ether
P	postnatal
PSS	photostationary state
PTX	picrotoxin
RP	reverse phase
s	second
TFA	trifluoroacetic acid
TCCA	trichloroisocyanuric acid
TTX	tetrodotoxin

#### REFERENCES

- (1) Korpi, E. R.; Sinkkonen, S. T. GABAA receptor subtypes as targets for neuropsychiatric drug development. *Pharmacol Ther* **2006**, *109*, 12–32.
- (2) Edwards, Z.; Preuss, C. V. GABA receptor positive allosteric modulators. In *StatPearls*; StatPearls Publishing, 2020.
- (3) George, K.; Preuss, C. V.; Sadiq, N. M. GABA inhibitors. In *StatPearls*; StatPearls Publishing, 2023.
- (4) Melzack, R.; Wall, P. D. Pain Mechanisms: A New Theory: A gate control system modulates sensory input from the skin before it evokes pain perception and response. *Science* **1965**, *150*, 971–979.
- (5) Zeilhofer, H. U.; Wildner, H.; Yévenes, G. E. Fast synaptic inhibition in spinal sensory processing and pain control. *Physiol Rev* **2012**, *92*, 193.
- (6) O'Connor, A. B.; Dworkin, R. H. Treatment of neuropathic pain: an overview of recent guidelines. *Am. J. Med.* **2009**, *122*, S22–S32.
- (7) Cruccu, G.; Truini, A. A review of neuropathic pain: from guidelines to clinical practice. *Pain Ther* **2017**, *6*, 35–42.
- (8) Kobauri, P.; Dekker, F. J.; Szymanski, W.; Feringa, B. L. Rational design in photopharmacology with molecular photoswitches. *Angew. Chem.* **2023**, *135*, No. e202300681.
- (9) Gomila, A. M. J.; Gorostiza, P. In Vivo Applications of Photoswitchable Bioactive Compounds. *Molecular Photoswitches: Chemistry, Properties, and Applications, 2 Volume Set* **2022**, 811–842.
- (10) Mukherjee, A.; Seyfried, M. D.; Ravoo, B. J. Azoheteroarene and Diazocine Molecular Photoswitches: Self-Assembly, Responsive



Materials and Photopharmacology. *Angew. Chem., Int. Ed.* **2023**, *62*, No. e202304437.

(11) Velema, W. A.; Szymanski, W.; Feringa, B. L. Photopharmacology: beyond proof of principle. *J. Am. Chem. Soc.* **2014**, *136*, 2178–2191.

(12) Schoenberger, M.; Damijonaitis, A.; Zhang, Z.; Nagel, D.; Trauner, D. Development of a new photochromic ion channel blocker via azologization of fomocaine. *ACS Chem. Neurosci.* **2014**, *5*, 514–518.

(13) Pittolo, S.; et al. An allosteric modulator to control endogenous G protein-coupled receptors with light. *Nat. Chem. Biol.* **2014**, *10*, 813–815.

(14) Matera, C.; et al. Photoswitchable antimetabolite for targeted photoactivated chemotherapy. *J. Am. Chem. Soc.* **2018**, *140*, 15764–15773.

(15) Kramer, R. H.; Rajappa, R. Interrogating the function of GABAA receptors in the brain with optogenetic pharmacology. *Curr. Opin Pharmacol* **2022**, *63*, No. 102198.

(16) Lin, W.-C.; et al. A comprehensive optogenetic pharmacology toolkit for in vivo control of GABAA receptors and synaptic inhibition. *Neuron* **2015**, *88*, 879–891.

(17) Davenport, C. M.; et al. Relocation of an extrasynaptic GABAA receptor to inhibitory synapses freezes excitatory synaptic strength and preserves memory. *Neuron* **2021**, *109*, 123–134.

(18) Yue, L.; et al. Robust photoregulation of GABAA receptors by allosteric modulation with a propofol analogue. *Nat. Commun.* **2012**, *3*, 1095.

(19) Borghese, C. M.; et al. Modulation of  $\alpha 1\beta 3\gamma 2$  GABAA receptors expressed in *X. laevis* oocytes using a propofol photoswitch tethered to the transmembrane helix. *Proc. Natl. Acad. Sci. U. S. A.* **2021**, *118*, No. e2008178118.

(20) Maleeva, G.; et al. A photoswitchable GABA receptor channel blocker. *Br. J. Pharmacol.* **2019**, *176*, 2661–2677.

(21) Mortensen, M.; Huckvale, R.; Pandurangan, A. P.; Baker, J. R.; Smart, T. G. Optopharmacology reveals a differential contribution of native GABAA receptors to dendritic and somatic inhibition using azogabazine. *Neuropharmacology* **2020**, *176*, No. 108135.

(22) Stein, M.; et al. Azo-propofols: photochromic potentiators of GABAA receptors. *Angew. Chem., Int. Ed.* **2012**, *51*, 10500–10504.

(23) Rustler, K.; et al. Optical Control of GABAA Receptors with a Fulgimide-Based Potentiator. *Chemistry A European Journal* **2020**, *26*, 12722–12727.

(24) Stephens, D. N. *Anxiolytic  $\beta$ -Carbolines: From Molecular Biology to the Clinic*; Springer Science & Business Media, 2013; Vol. 11.

(25) Stephens, D. N.; et al. Abecarnil, a metabolically stable, anxiolytic beta-carboline acting at benzodiazepine receptors. *J. Pharmacol Exp Ther.* **1990**, *253*, 334–343.

(26) Pribilla, I. et al. Abecarnil is a full agonist at some, and a partial agonist at other recombinant GABAA receptor subtypes. *Anxiolytic  $\beta$ -carbolines: from molecular biology to the clinic*; Stephens, D. N., Eds.; Psychopharmacology Series; Springer: Berlin, Heidelberg, 1993; Vol 11, pp 50–61.

(27) Ozawa, M.; et al. Pharmacological characterization of the novel anxiolytic  $\beta$ -carboline abecarnil in rodents and primates. *Japanese Journal of Pharmacology* **1994**, *64*, 179–187.

(28) Barbaccia, M. L.; et al. Stress-induced increase in brain neuroactive steroids: antagonism by abecarnil. *Pharmacol., Biochem. Behav.* **1996**, *54*, 205–210.

(29) Aufdembrinke, B. Abecarnil, a new beta-carboline, in the treatment of anxiety disorders. *British Journal of Psychiatry* **1998**, *173*, 55–63.

(30) Sigel, E.; Ernst, M. The benzodiazepine binding sites of GABAA receptors. *Trends Pharmacol. Sci.* **2018**, *39*, 659–671.

(31) Yarom, M.; et al. Identification of inosine as an endogenous modulator for the benzodiazepine binding site of the GABAA receptors. *J. Biomed Sci.* **1998**, *5*, 274–280.

(32) MacDonald, J. F.; Barker, J. L.; Paul, S. M.; Marangos, P. J.; Skolnick, P. Inosine may be an endogenous ligand for benzodiazepine

receptors on cultured spinal neurons. *Science* (1979) **1979**, *205*, 715–717.

(33) Stephens, D. N.; Turski, L.; Jones, G. H.; Steppuhn, K. G.; Schneider, H. H. Abecarnil: a novel anxiolytic with mixed full agonist/partial agonist properties in animal models of anxiety and sedation. *Anxiolytic  $\beta$ -Carbolines: From Molecular Biology to the Clinic* **1993**, 79–95.

(34) Zhu, S.; et al. Structural and dynamic mechanisms of GABAA receptor modulators with opposing activities. *Nat. Commun.* **2022**, *13*, 4582.

(35) Kim, J. J.; et al. Shared structural mechanisms of general anaesthetics and benzodiazepines. *Nature* **2020**, *585*, 303–308.

(36) Kelly, M. D.; et al. Role of the histidine residue at position 105 in the human  $\alpha 5$  containing GABAA receptor on the affinity and efficacy of benzodiazepine site ligands. *Br. J. Pharmacol.* **2002**, *135*, 248–256.

(37) Masiulis, S.; et al. GABAA receptor signalling mechanisms revealed by structural pharmacology. *Nature* **2019**, *565*, 454–459.

(38) Crestani, F.; Assandri, R.; Täuber, M.; Martin, J. R.; Rudolph, U. Contribution of the  $\alpha 1$ -GABAA receptor subtype to the pharmacological actions of benzodiazepine site inverse agonists. *Neuropharmacology* **2002**, *43*, 679–684.

(39) Kasaragod, V. B.; et al. The molecular basis of drug selectivity for  $\alpha 5$  subunit-containing GABAA receptors. *Nat. Struct. Mol. Biol.* **2023**, *30*, 1936–1946.

(40) Ramerstorfer, J.; Furtmüller, R.; Vogel, E.; Huck, S.; Sieghart, W. The point mutation  $\gamma 2F77I$  changes the potency and efficacy of benzodiazepine site ligands in different GABAA receptor subtypes. *Eur. J. Pharmacol.* **2010**, *636*, 18–27.

(41) Nin-Hill, A.; Mueller, N. P. F.; Molteni, C.; Rovira, C.; Alfonso-Prieto, M. Photopharmacology of Ion channels through the light of the computational microscope. *Int. J. Mol. Sci.* **2021**, *22*, 12072.

(42) Buhr, A.; Baur, R.; Sigel, E. Subtle changes in residue 77 of the  $\gamma$  subunit of  $\alpha 1\beta 2\gamma 2$  GABAA receptors drastically alter the affinity for ligands of the benzodiazepine binding site. *J. Biol. Chem.* **1997**, *272*, 11799–11804.

(43) Whiting, P. J. GABA-A receptor subtypes in the brain: a paradigm for CNS drug discovery? *Drug Discov Today* **2003**, *8*, 445–450.

(44) Qian, X.; et al. Current status of GABA receptor subtypes in analgesia. *Biomedicine & Pharmacotherapy* **2023**, *168*, No. 115800.

(45) Foster, E.; et al. Targeted ablation, silencing, and activation establish glycinergic dorsal horn neurons as key components of a spinal gate for pain and itch. *Neuron* **2015**, *85*, 1289–1304.

(46) Theruveethi, N. Impact of light-emitting diodes on visual cortex layer 5 pyramidal neurons (VI-LSPNs)—A rodent study. *Mol. Vis* **2024**, *30*, 67.

(47) Rodrigues, R. B.; et al. Dithiothreitol reduces oxidative stress and necrosis caused by ultraviolet A radiation in L929 fibroblasts. *Photochemical & Photobiological Sciences* **2024**, *23*, 271–284.

(48) Vorobjev, V. S.; Sharonova, I. N.; Skrebitsky, V. G.; Schneider, H. H.; Stephens, D. N. Abecarnil enhances GABA-induced currents in acutely isolated cerebellar Purkinje cells. *Neuropharmacology* **1995**, *34*, 157–163.

(49) McAdam, L. C. Propofol and benzodiazepine modulation of GABA (A) R function. *Thesis*, 1998.

(50) Thomet, U.; Baur, R.; Scholze, P.; Sieghart, W.; Sigel, E. Dual mode of stimulation by the  $\beta$ -carboline ZK 91085 of recombinant GABAA receptor currents: molecular determinants affecting its action. *Br. J. Pharmacol.* **1999**, *127*, 1231–1239.

(51) Iorio, M. T.; et al. GABAA receptor ligands often interact with binding sites in the transmembrane domain and in the extracellular domain—can the promiscuity code be cracked? *Int. J. Mol. Sci.* **2020**, *21*, 334.

(52) Martínez, A. L.; et al. In Vitro Models for Neuropathic Pain Phenotypic Screening in Brain Therapeutics. *Pharmacol. Res.* **2024**, *202*, No. 107111.

(53) Hüll, K.; et al. Optical control of adenosine-mediated pain modulation. *Bioconjug Chem.* **2021**, *32*, 1979–1983.

(54) Pereira, V.; Arias, J. A.; Llebaria, A.; Goudet, C. Photopharmacological manipulation of amygdala metabotropic glutamate receptor mGlu4 alleviates neuropathic pain. *Pharmacol. Res.* **2023**, *187*, No. 106602.

(55) Zussy, C.; et al. Dynamic modulation of inflammatory pain-related affective and sensory symptoms by optical control of amygdala metabotropic glutamate receptor 4. *Mol. Psychiatry* **2018**, *23*, 509–520.

(56) Ricart-Ortega, M.; et al. Mechanistic insights into light-driven allosteric control of GPCR biological activity. *ACS Pharmacol Transl Sci.* **2020**, *3*, 883–895.

(57) Gómez-Santacana, X.; et al. Illuminating phenylazopyridines to photoswitch metabotropic glutamate receptors: from the flask to the animals. *ACS Cent Sci.* **2017**, *3*, 81–91.

(58) Camerin, L.; et al. Photoswitchable Carbamazepine Analogs for Non-Invasive Neuroinhibition In Vivo. *Angew. Chem.* **2024**, No. e202403636.

(59) Dong, M.; Babalhavaeji, A.; Samanta, S.; Beharry, A. A.; Woolley, G. A. Red-shifting azobenzene photoswitches for in vivo use. *Acc. Chem. Res.* **2015**, *48*, 2662–2670.

(60) Krause, W.; Schütt, B.; Duka, T. Pharmacokinetics and acute toleration of the beta-carboline derivative abecarnil in man. *Arzneimittelforschung* **1990**, *40*, 529–532.

(61) Trenité, D. G. A. K.-N.; Groenwold, R. H. H.; Schmidt, B.; Löscher, W. Single dose efficacy evaluation of two partial benzodiazepine receptor agonists in photosensitive epilepsy patients: a placebo-controlled pilot study. *Epilepsy Res.* **2016**, *122*, 30–36.